Full Length Research Paper

Intramolecular proton transfer of 2-[(2,4-dimethylphenyl)iminomethyl]-3,5-dimethoxyphenol Schiff-base ligand: A density functional theory (DFT) study

S. Ali Beyramabadi* and Ali Morsali

Department of Chemistry, Mashhad Branch, Islamic Azad University, Mashhad, Iran.

The title Schiff-base ligand could exist as two enol-imino (E) and keto-enamine (K) tautomers. Here, employing density functional theory, and handling the solvent effects with the polarizable continuum model (PCM), the structural parameters, energetic behavior, natural bond orbital analysis, as well as tautomerization mechanism of the E and K tautomers are investigated. The percentage of tautomers and activation energy of the tautomerization reaction have been computed in the gas and solution phases. In the gas phase, the E form is dominant, whereas considering the solvent effect prefers the K tautomer in the polar solvents. The tautomerization reaction includes an intramolecular-proton transfer, which affects considerably the structural parameters as well as atomic charges of the ligand. The presented model leads to results which have good consistency with the experimental and theoretical evidence.

Key words: Density functional theory, polarizable continuum model (PCM), enol-keto tautomerism, intramolecular proton transfer, Schiff base.

INTRODUCTION

Study on the Schiff-base compounds is of great importance from different aspects, the most significant of which are: existence of inter- and intramolecular-hydrogen-bonding interactions in their structures (Lin and Gao, 2010; Gallant et al., 2005; Fabian et al., 2004; Görner et al., 2006), versatile metal bonding ability (Görner et al., 2006; Toscano and Marzilli, 1984; Valent et al., 2002; Wang et al., 2009), biological activities (Lin and Gao, 2010; Bottcher et al., 1997; Liu et al., 2001; Hodnett and Mooney, 2001) and industrial uses as catalyst (Gupta and Sutar, 2007, 2008; Baleizão and Garcia, 2006) and dyes (Taggi et al., 2002). Also, one of the most important features of the Schiff bases is intramolecular-proton transfer (IPT), which has attracted ever increasing attention in recent years (Lin and Gao, 2010; Gallant et

al., 2005; Fabian et al., 2004; Kluba et al., 2008; Jezierska-Mazzarello, 2010; Bach et al., 1999; Sauer et al., 2006; Rodríguez-Córdoba et al., 2007; Rospenk et al., 2003).

The ortho-hydroxy aromatic Schiff-base ligands could exist as two tautomeric forms: enol-imino (E) and keto-enamine (K). Tautomerism in these compounds was widely investigated by using experimental and theoretical methods (Lin and Gao, 2010; Görner et al., 2006; Kluba et al., 2008; Jezierska-Mazzarello, 2010; Bach et al., 1999; Sauer et al., 2006; Rodríguez-Córdoba et al., 2007; Rospenk et al., 2003; Dudek and Dudek, 1966; Upadhyay et al., 2008; Tezer and Karakus, 2009; Tanak and Yavuz, 2009). In the solid state, salicylideneaniline Schiff bases exist in the E form (Görner et al., 2006; Nazir et al., 2000; Elmali et al., 1998; Ersanli et al., 2004; Temel et al., 2007; Gül et al., 2007; Sahin et al., 2009; Tanak et al., 2009; Kelesoglu et al., 2009; Tanak et al., 2009). The H-atom transfer from hydroxyl O atom to the imine N atom causes to interesting photochromic and thermochromic behaviors. Hence, these compounds can be used in

---
*Corresponding author. E-mail: beiramabadi6285@mshdiau.ac.ir, morsali@mshdiau.ac.ir. Tel: +98 511 8414182. Fax: +98 511 8414182.

molecular electronic and optical data storage devices (Alarcon et al., 1999; Feringa et al., 1993; Hadjoudis and Mavridis, 2004; Ziółek et al., 2008).

Now, the density functional theory (DFT) as a remarkable method is widely used in many areas of the computational chemistry, such as kinetics and mechanism investigations of the reactions, spectroscopic assignments, characterization of the molecular structures, and so on (Lin and Gao, 2010; Fabian et al., 2004; Jezierska-Mazzarello, 2010; Bach et al., 1999; Upadhyay et al., 2008; Tezer and Karakus, 2009; Tanak and Yavuz, 2009; Chowdhury et al., 2010; Abdel-Hafiez et al., 2010; Beyramabadi et al., 2008, 2009; Eshtiagh-Hosseini et al., 2008, 2010; Pishkar et al., 2010; Emampour et al., 2009).

Recently, Tanak et al. (2009) reported the x-ray structure of the title Schiff-base ligand. The x-ray analysis showed that both E and K tautomers of the ligand coexist with occupancies of 62 (3) and 38 (3)%, respectively.

Previously, no theoretical study has been reported on the title compound. In this work, we have theoretically investigated the geometrical structures and energy contents of both E and K tautomers of the title compound, as well as the mechanism of tautomerization reaction in the gas and solution phases. In addition, the natural bond orbital (NBO), charge on the atoms and the frontier molecular orbital (FMO) analysis were performed.

THEORETICAL METHODS

All of the present calculations have been performed with the Gaussian 98 software package (Frisch et al., 1998) by using the B3LYP hybrid functional (Beck's three parameter hybrid functional using the LYP correlation functional) (Lee et al., 1988) and the 6-311+G(d,p) basis set.

First, all degrees of freedom for all geometries were optimized. The optimized geometries were confirmed to have no imaginary frequency, except for transition state (TS) that has only one imaginary frequency of the Hessian. The frequency calculations were also performed for the evaluation of the zero-point energies and the Gibbs free energies. In the gas phase, the zero-point corrections were considered to obtain energies.

Here, one of self-consistent reaction field methods, the sophisticated polarizable continuum model (PCM) (Tomasi and Cammi, 1995) has been employed for investigation of solute-solvent interactions. The gas phase optimized geometries were used to apply the solvent effects, where ethanol, water and chloroform have been considered as solvent. The atomic charges, the NBO and FMO analysis were performed on the optimized structures.

RESULTS AND DISCUSSION

Optimized geometries of the E and K tautomers

X-ray analysis showed that the crystal structure of the title compound is monoclinic. The compound involves both E and K tautomers in its molecular structure (Tanak et al., 2009). In this work, geometries of both the tautomers have been fully optimized in vacuum. Some of the calculated structural parameters are gathered in Table 1, together with the experimental corresponding values. As seen, the calculated structural parameters are in good agreement with the x-ray experimental ones (Tanak et al., 2009).

The optimized geometries of the K and E tautomers are shown in Figure 1. The structure of K form is more planar than the E form one. The calculated C10-C13-C2-C5 and C9-C13-C2-C6 dihedral angles are 145.34 and 138.70° for the E form, and 167.15 and 163.88° for the K form, respectively. The planarity of the structures can be attributed to the strong intramolecular-hydrogen-bond interaction, which locks the salicyldimine moiety (Tezer and Karakus, 2009). This interaction give rises to a six-membered ring in both the E and K tautomers. In the E tautomer, the intramolecular H-bonding is between O-H donor and imine N acceptor, but in the case of the K tautomer, the interaction is between N-H donor and phenolic O1 acceptor. The N4H1a…O1 bond length in the K form, and O1H1a…N4 bond length in the E form are 1.7074 and 1.6801 Å, respectively. Therefore, the H-bonding interaction in the E form is stronger than the K form, which is in agreement with the experimental (Tanak et al., 2009) and similar theoretical (Jezierska-Mazzarello et al., 2010; Upadhyay et al., 2008) evidence. The experimental H-bond lengths of the E and K forms are 1.821 and 1.861 Å, respectively. The calculated D-H1a A hydrogen-bond angles in the E and K tautomers are 149.12 and 139.67°, respectively, and their corresponding experimental values are 149.0 and 137.1°, respectively. Also, the calculated O1-N1 distances of the E and K tautomers are 2.5922 and 2.5878 Å, respectively, which are in good agreement with the experimental value (2.5612 Å).

Due to the E→K IPT, a number of structural parameters of the E form have changed, the most important of which have been presented subsequently. The K form is more planar than the E form (Table 1). The C2-O1 bond length decreases from 1.3374 to 1.2614 Å in the K form, which is between the phenolic C-O single bond length (1.330 Å) and double C=O bond length (1.210 Å). Going from the E to the K tautomer, the C1-C7 bond length decreases form 1.4421 to 1.3898 Å, whereas the C7-N1 bond length enlarges from 1.2946 to 1.3339 Å. In the generated six-membered ring, which involves the intramolecular hydrogen bond, the C-O, C-C and C-N bond lengths are between the corresponding length of single bond and that of a double bond, indicating formation of a conjugation system in this region of both the E and K tautomers of the title Schiff-base ligand. The obtained results are in agreement with the previously reported data for similar compounds (Gallant et al., 2005; Jezierska-Mazzarello et al., 2010; Tezer and Karakus, 2009; Elmali et al., 1998; Ersanli et al., 2004; Temel et al., 2007; Gül et al., 2007, Sahin et al., 2009; Tanak et al., 2009; Kelesoglu et al., 2009; Tanak et al., 2009).

Tautomerization mechanism

Here, the tautomerization mechanism of the title ligand

Table 1. Selected theoretical structural parameters for the studied species together with the corresponding experimental values for comparison.

	Theoretical			Experimental
	E form	**K form**	**TS1**	
Bond length (Å)				
N1-H1a	1.6801	1.0384	1.3258	1.823 0.8589
O1-H1a	1.0026	1.7074	1.1488	1.8672 0.8200
C2-O1	1.3374	1.2614	1.3085	1.3314
C1-C2	1.4186	1.4705	1.4347	1.4063
C2-C3	1.4005	1.4347	1.4100	1.3972
C3-C4	1.3886	1.3725	1.3849	1.3687
C4-C5	1.4081	1.4300	1.4157	1.3991
C5-C6	1.3829	1.3671	1.3785	1.3673
C6-C1	1.4234	1.4410	1.4245	1.4162
C6-O2	1.3618	1.3624	1.3617	1.3665
O2-C16	1.4232	1.4234	1.4246	1.4229
C4-O3	1.3584	1.3579	1.3582	1.3634
O3-C17	1.4244	1.4247	1.4246	1.4270
C1-C7	1.4421	1.3898	1.4226	1.4264
C7-N1	1.2946	1.3339	1.3086	1.2922
N1-C8	1.4083	1.4082	1.4074	1.4166
C8-C9	1.4117	1.4099	1.4116	1.3955
C9-C10	1.3943	1.3954	1.3944	1.3914
C10-C11	1.4000	1.3977	1.3996	1.3763
C11-C12	1.3959	1.3971	1.3961	1.3805
C12-C13	1.3915	1.3897	1.3909	1.3848
C9-C14	1.5077	1.5087	1.5078	1.5058
C11-C15	1.5097	1.5093	1.5095	1.5098
O1-N1	2.5922	2.5878	2.4151	2.5612
Angle (°)				
N1-H1a-O1	149.12	139.67	154.76	149.0 137.1
H1a-O1-C2	107.16	104.55	104.43	109.44 101.17
O1-C2-C1	120.88	120.84	119.54	120.65
C2-C1-C7	121.33	120.66	118.85	121.48
C1-C7-N1	120.08	122.96	119.64	121.77
C7-N1-C8	120.87	127.50	123.99	123.92
N1-C8-C9	118.52	118.18	118.36	116.93
C8-C9-C14	120.77	121.22	121.92	120.81
C4-O3-C17	118.79	118.62	118.79	116.69
C6-O2-C16	118.96	118.59	118.71	117.08
C10-C11-C15	120.83	121.09	120.78	121.57
Dihedral angle (°)				
H1a-O1-C2-C1	-0.01	-0.29	-0.15	-0.78 -1.67

Table 1. Contd.

H1a-N1-C7-C1	0.42	-1.36	-0.46	0.84 -1.56
C1-C2-C4-C5	-0.18	-0.30	-0.18	-0.29
C9-C10-C12-C13	0.30	-0.30	0.13	0.38(5)
C10-C13-C2-C5	145.34	167.15	-154.84	173.15
C9-C13-C2-C6	138.70	163.88	-148.94	173.06
C5-C6-O2-C16	0.34	0.05	0.32	3.46
C3-C4-O3-C17	-0.28	-0.39	-0.38	-1.29
C2-C1-C7-N1	-0.72	0.29	0.11	1.82
C11-C10-C9-C14	179.87	-179.63	-179.93	178.15
C9-C10-C11-C15	-178.15	-178.57	-178.99	179.02

E tautomer
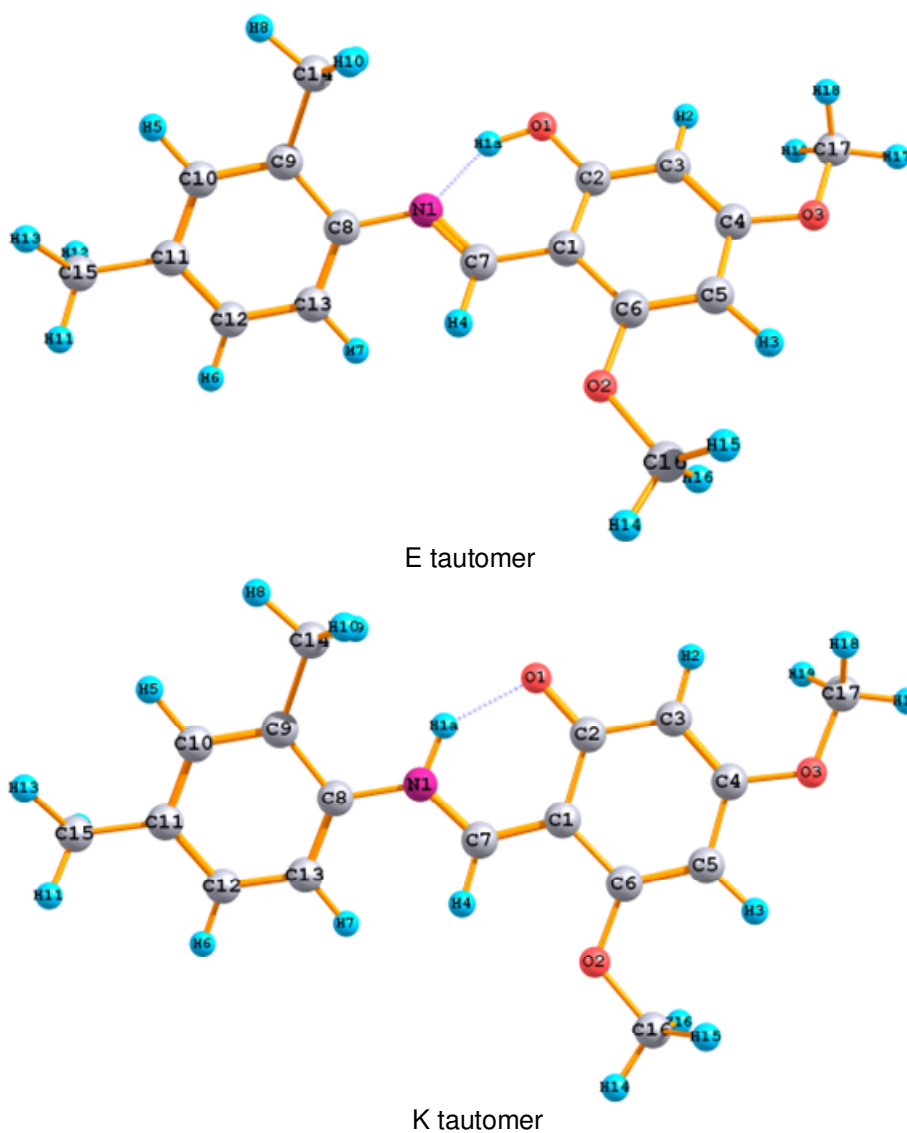
K tautomer

Figure 1. The B3LYP/6-311+G(d,p) optimized structures of the enol-imino (E) and keto-enamine (K) tautomers of the title compound.
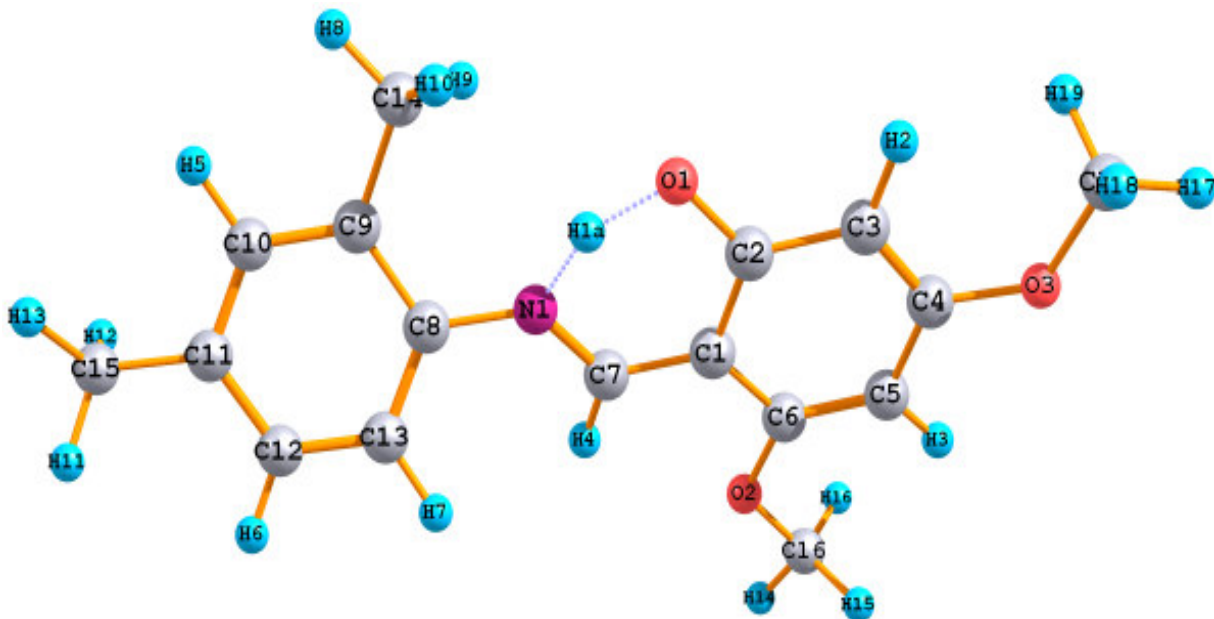
Figure 2. The B3LYP/6-311+G(d,p) optimized structure of the transition state (TS1) of the E-K tautomerization.

has been theoretically investigated. The obtained TS was confirmed to have only one imaginary frequency. The obtained structure for the TS (TS1) is shown in Figure 2, which is roughly planar (Table 1). In the optimized structure of TS1, breaking of the O1-H1a bond together with the formation of N1-H1a bond is clear. The O1-H1a and N1-H1a distances vary from 1.0026 and 1.6801 Å for the E tautomer to 1.1488 and 1.3258 Å for the TS1, respectively. These distances are 1.7074 and 1.0384 Å for the K tautomer, respectively. During the E→TS1→K H-transfer process, the O1-H1a and C7-N1 distances increase, while the N1-H1a and C1-C7 distances decrease.

Tautomerization energies and solvent effects

Here, the tautomerization energies were computed in the gas and solution phases. The solvent plays important role in chemical reactions. The used PCM model is a valuable approach for investigation of the solute-solvent interactions, so it is widely used in theoretical studies of the chemical reactions (Kluba et al., 2008; Chowdhury et al., 2010; Abdel-Hafiez et al., 2010; Beyramabadi et al., 2008, 2009; Eshtiagh-Hosseini et al., 2010; Pishkar et al., 2010).

In the gas phase, the E tautomer is more stable than the K one, leading to an endothermic E→K tautomerization by 1.13 kcal/mol. In contrast, this tautomerization has an exothermicity of -0.50 kcal/mol in the ethanol solution. For the E→K tautomerization, E_as in the gas phase and PCM model are 3.11 and 3.58

kcal/mol, respectively. Because of the lowest dipole moment for the TS2, the E_a of the tautomerism reaction increases in the ethanol solution compared to the gas phase.

Considering solvent effects stabilizes all the species. The dipole moments increase during the E-K tautomerization, and larger dipole moment leads to larger stabilization effect with respect to the gas phase calculations. The computed dipole moments for the E, K and TS1 species are 2.4593, 2.6628 and 2.2671 D, respectively. Hence, the order of solvation energies is K>E>TS1, which result in an exothermic E→K tautomerization reaction in solution with higher energy barrier than the gas phase.

Considering the equilibrium between the E and K tautomers, the value of the tautomeric equilibrium constant (K) is calculated by using

$$K = \exp(-\frac{\Delta G}{RT}) \tag{1}$$

where ΔG, R and T are the Gibbs free energy difference between the two tautomers, the gas constant and temperature, respectively.

The gas phase Gibbs free energy difference between the tautomers is 0.49 kcal/mol, in favor of the E tautomer. Hence, using the Equation (1), the amount of the K form is predicted to be 30.43%, which is consistent with the experimental value (38.3% for the K form) (Tanak et al., 2009). Their difference can be attributed to the intermolecular interactions in the solid state, which

Table 2. The natural charges for the atoms of the E and K tautomers of the title compound and TS1 species.

Atom	NBO atomic charges		
	E form	TS1	K form
H1a	0.4462	0.5069	0.3773
N1	-0.0390	-0.1017	-0.0234
O1	-0.4058	-0.5039	-0.5048
O2	-0.2088	-0.2170	-0.2162
O3	-0.2258	-0.2205	-0.2195
C1	0.8614	0.6697	0.7753
C2	-0.1578	-0.5092	-0.6579
C7	0.1027	0.1261	0.3572

are neglected in the gas phase calculations for the isolated molecule. But, in the solution phase, the K form has lower Gibbs free energy than the E one. The calculated ∆G is 0.59 kcal/mol, which proposes that amount of the K form is 73.02% in ethanol.

Decreasing of the solvent polarity favors the E form in comparison with the K form. So, going from water to ethanol and chloroform solvents, percentage of the K form in solution decreases from 74.34 to 73.02 and 47.47%, respectively. Also, in these solvents the E_a of the E$\rightarrow$K tautomerization decreases from 3.59 to 3.58 and 3.57 kcal/mol, respectively.

NBO analysis

In this work, the NBO calculations have been performed at the B3LYP/6-311+G(d,p) level. The NBO analysis is a useful method for studying intra- and intermolecular bonding interactions and investigation of charge transfer in chemical compounds (Snehalatha et al., 2009).

The NBO atomic charges of the E and K tautomers and TS1 species are selectively gathered in Table 2. We have investigated the charge population on the H1a, O1 and N1 atoms, which contribute directly in the H-transferring process. In the solution phase, the computed charges indicate a high positive charge on the H1a atom during the E-K tautomerization, displaying an IPT between the O1 and N1 atoms. Due to the IPT, a number of atomic charges change, the most important of which are presented subsequently.

As expected, during the E$\rightarrow$K IPT, the negative charge of the donor oxygen O1 increases, whereas that of the acceptor nitrogen N1 atom decreases. The positive charge on the transferring hydrogen (H1a) for the E form is higher than the K form (Table 2).

The NBO charge population indicates that in ethanol solution, the positive charge of the H1a is higher than the gas phase, leading to easier formation of the anionic ligand and H^+ species in the solution. Compared to the E form, in the K form, the C7=N1 π-electrons are engaged

in formation of N-H amine bond, inducing larger positive charge on the C7 atom.

The amount of stabilization energy of hyper conjugative interactions (E(2)), resulting from electron delocalization between donor NBO(*i*) and acceptor NBO(*j*) orbitals is a criteria for determining the degree of interaction between electron donor and electron acceptor (orbitals). The greater the E(2), the greater electron transferring tendency from electron donor to electron acceptor, resulting to more electron density delocalization, and consequently leading to more stabilization of the system. The value of E(2) is calculated by using (Schwenke and Truhlar, 1985; Gutowski and Chalasinski, 1993)

$$E(2) = -q_i \frac{(F_{ij})^2}{\varepsilon_j - \varepsilon_i} \qquad (2)$$

where q_i, F_{ij}, ε_j and ε_i parameters are the donor orbital occupancy, the off-diagonal NBO Fock matrix element, energies of the acceptor and donor orbitals, respectively.

The lower ε_j-ε_i energy difference the higher the E(2) stabilization energy. The parameters of Equation (2) have been obtained from the second-order perturbation theory analysis of Fock matrix in NBO basis. The selected results are given in Table 3.

In both tautomers, the strong $n(O1) \rightarrow \sigma^*(C1\text{-}C2)$ interaction induces high stabilization energy, which elongates the C1-C2 bond to such an extent that it becomes the longest aromatic C-C bond in the 3,5-dimethoxyphenolic moiety. The electron donations result in a conjugation of the six-membered ring with the phenyl ring.

Electron donation from lone pair of the N4 to the σ-antibonding orbital of the O1-H1a has a quite large E(2), stabilizes the E tautomer by 30.16 kcal/mol, either increasing the strength of the intramolecular O1-H1a...N4 hydrogen bond. For the K tautomer, the strongest

Table 3. The second-order perturbation theory analysis of Fock matrix in natural bond orbital (NBO) basis for the E and K tautomers.

Donor NBO (i)	Acceptor NBO (j)	ε_j-ε_i (a.u.)[a]	F_{ij} (a.u.)[b]	E(2) (kcal/mol)[c]
E tautomer				
LP(1) O1	BD*(1) C1-C2	1.11	0.076	6.50
LP(2) O1	BD*(2) C1-C2	0.32	0.109	39.62
LP(1) O2	BD*(1) C16-H35	0.93	0.047	2.89
LP(2) O2	BD*(1) C16-H36	0.69	0.057	5.48
LP(2) O2	BD*(1) C16-H37	0.69	0.057	5.47
LP(1) O3	BD*(1) C17-H38	0.93	0.047	2.91
LP(2) O3	BD*(1) C17-H39	0.69	0.057	5.47
LP(2) O3	BD*(1) C17-H40	0.69	0.057	5.42
LP(1) N4	BD*(1) O1-H1a	0.76	0.137	30.16
LP(1) N4	BD*(1) C1-C11	0.85	0.046	2.86
LP(1) N4	BD*(1) C11-H25	0.76	0.081	10.19
K tautomer				
LP(1) O1	BD*(1) N4-H1a	1.03	0.062	4.57
LP(2) O1	BD*(1) N4-H1a	0.67	0.107	20.91
LP(2) O1	BD*(1) C1-C2	0.76	0.084	11.13
LP(1) O2	BD*(1) C16-H35	0.93	0.046	2.85
LP(2) O2	BD*(1) C16-H36	0.69	0.057	5.45
LP(2) O2	BD*(1) C16-H37	0.69	0.057	5.44
LP(1) O3	BD*(1) C17-H38	0.93	0.047	2.88
LP(2) O3	BD*(1) C17-H39	0.69	0.057	5.40
LP(2) O3	BD*(1) C17-H40	0.69	0.057	5.35

[a] Energy difference between donor (i) and acceptor (j) NBO orbitals. [b] Fock matrix element between i and j NBO orbitals. [c] Energy of hyper conjugative interactions.

electron donation is related to n(O1) $\rightarrow \sigma^*$ (N4-H1a) NBO interaction, leading to the strong intramolecular N4-H1a...O1 hydrogen bond.

As can be seen from Table 3, the weak n(O) $\rightarrow \sigma^*$ (C-H) NBO interactions demonstrate the existence of C-H...O hydrogen bonds, with their stabilizing energies are between 2.85 to 5.48 kcal/mol. Also, in the E form, there is a relative strong n(N4) $\rightarrow \sigma^*$ (C11-H25) interaction by 10.19 kcal/mol as the stabilizing energy, indicating a C11-H25...N4 hydrogen bonding interaction.

The distributions and energy levels of the frontier orbitals for the E and K tautomers of the title compound have been shown in Figure 3. As seen, the highest occupied molecular orbitals (HOMOs) of both tautomers are mainly localized on the whole of tautomeric structures exception for the substituted groups on the phenyl rings. But, the lowest-lying unoccupied molecular orbitals (LUMOs) are mainly localized on the phenyl ring of the 3,5-dimethoxyphenolic moiety and the C1-C7-N1-C8 fragment in both tautomers.

The energy difference between the HOMO and LUMO frontier orbitals is one of the important characteristics of molecules, which has a determining role in such cases as electric properties, electronic spectra and photochemical reactions. The values of the energy separation between the HOMO and LUMO are 3.63 and 4.07 ev for the K and E tautomers, respectively. These large energy gaps imply that structure of the title Schiff-base ligand is very stable (Tezer and Karakus, 2009; Özdemir et al., 2009).

Conclusions

Structural parameters and energetic characters of both E and K tautomers of the title Schiff-base ligand, as well as its tautomerization mechanism have been theoretically studied in detail in the gas and PCM model. The DFT calculations show that the E tautomer is more stable than the K tautomer in the gas phase, while solute-solvent interactions favor the K tautomer in ethanol. The energy barriers of the E $\rightarrow$ K tautomerization in the gas and solution phases are predicted to be 3.11 and 3.58 kcal/mol, respectively. In the gas phase, the ΔG between the E and K tautomers is equal to 0.49 kcal/mol, resulting in the value of K form to be 30.43%, which is in agreement with the experimental evidence. The results obtained from PCM Model shows that the percentage of K form in the solution is 73.02%.

E-HOMO

K-HOMO

E-LUMO

K-LUMO
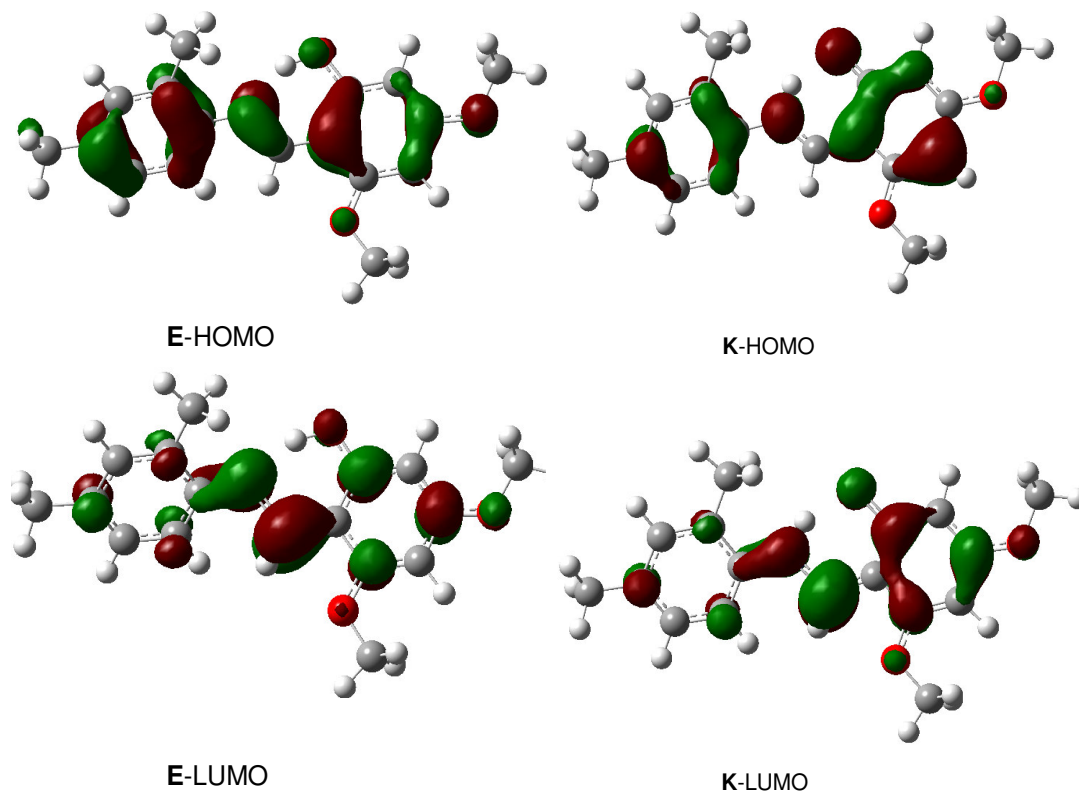
Figure 3. The HOMO and LUMO frontier orbitals of the E and K tautomers.

The computed atomic charges support an intramolecular-proton transfer during the tautomerization. In the solution phase, the positive charge of the transferring H atom is larger than the gas phase. The NBO electron donations cause to a conjugation system, increasing stability of the title compound. In addition, for both E and K tautomers, the energy gap between the HOMO and LUMO orbitals is large.

ACKNOWLEDGEMENT

REFERENCES

Abdel-Hafiez A, Atteya R, Medhat ME (2010). Theoretical investigations for electronic structures and photodissociation of bromine molecule. Int. J. Phys. Sci., 5(7): 978-983.

Alarcon SH, Pagani D, Bacigalupo J, Olivieri AC (1999). Spectroscopic and semiempirical MO study of substituent effects on the intramolecular proton transfer in anils of 2-hydroxy-benzaldehydes. J. Mol. Struct., 475: 233-240.

Bach RD, Canepa C, Glukhovtsev MN (1999). Influence of Electrostatic Effects on Activation Barriers in Enzymatic Reactions: Pyridoxal 5´-Phosphate-Dependent Decarboxylation of α-Amino Acids. J. Am. Chem. Soc., 121(28): 6542-6555.

Baleizão C, Garcia H (2006). Chiral Salen Complexes: An Overview to Recoverable and Reusable Homogeneous and Heterogeneous

Catalysts. Chem. Rev., 106(9): 3987-4043.

Beyramabadi SA, Eshtiagh-Hosseini H, Housaindokht MR, Morsali A (2008). Mechanism and Kinetics of the Wacker Process: A Quantum Mechanical Approach. Organometallics, 27(1): 72-79.

Beyramabadi SA, Eshtiagh-Hosseini H, Housaindokht MR, Morsali A (2009). H-Transfer steps of the Wacker process: A DFT study. J. Mol. Struct. Theochem., 903(1-3): 108-114.

Bottcher A, Takeuchi Y, Hardcastle KI, Meade TJ, Gray HB (1997). Spectroscopy and Electrochemistry of Cobalt(III) Schiff Base Complexes. Inorg. Chem., 36(12): 2498-2504.

Chowdhury S, Himo F, Russo N, Sicilia E (2010). Mechanistic Investigation of the Hydrogenation of O_2 by a Transfer Hydrogenation Catalyst. J. Am. Chem. Soc., 132(12): 4178-4190.

Dudek GO, Dudek EP (1966). Spectroscopic Studies of Keto-Enol Equilibria. IX. N15-Substituted Anilides. J. Am. Chem. Soc., 88(11): 2407-2412.

Elmali A, Elerman Y, Kendi E (1998). N-(2-Bromo-4-methylphenyl)naphthaldimine. Acta Cryst., C54: 1137-1139.

Emampour JS, Morsali A, Beyramabadi SA (2009). The heat capacities from analytical distribution functions. J. Theo. Comput. Chem., 8(1): 943-956.

Ersanli CC, Odabasoglu M, Albayrak Ç, Erdönmez A (2004). 2-[2-(Hydroxymethyl)phenyliminomethyl]phenol. Acta Cryst., E60: o264-o266.

Eshtiagh-Hosseini H, Beyramabadi SA, Housaindokht MR, Morsali A (2010). O-H bond cleavage step of the Wacker process: A DFT study. J. Mol. Struct. Theochem., 941(1-3): 138-143.

Eshtiagh-Hosseini H, Housaindokht MR, Beyramabadi SA, Beheshti S, Esmaeili AA, Javan-Khoshkholgh M, Morsali A (2008). Synthesis, experimental and theoretical characterization of tetra dentate N,N′-dipyridoxyl (1,3-propylenediamine) salen ligand and its Co(III) complex. Spectrochim. Acta. Part A., 71(4): 1341-1347.

Fabian WMF, Antonov L, Nedeltcheva D, Kamounah FS, Taylor PJ (2004). Tautomerism in Hydroxynaphthaldehyde Anils and Azo

Analogues: A Combined Experimental and Computational Study. J. Phys. Chem., A 108(37): 7603-7612.

Feringa BL, Jager WF, De Lange B (1993). Organic materials for reversible optical data storage. Tetrahedron, 49(37): 8267-8310.

Frisch MJ (1998). Gaussian 98, Revision A.7; Gaussian, Inc.: Pittsburgh PA,

Gallant AJ, Yun M, Sauer M, Yeung CS, MacLachlan MJ (2005). Tautomerization in Naphthalenediimines: A Keto-Enamine Schiff Base Macrocycle. Org. Lett., 7(22): 4728-4830.

Görner H, Khanra S, Weyhermüller T, Chaudhuri P (2006). Photoinduced Intramolecular Proton Transfer of Phenol-Containing Ligands and Their Zinc Complexes. J. Phys. Chem. A., 110(8): 2587-2594.

Gül ZS, Ersahin F, Agar E, Isik S (2007). (E)-4-Bromo-2-(2-methoxyphenyliminomethyl)phenol. Acta Cryst. E63: o4241.

Gül ZS, Ersahin F, Agar E, Isik S (2007). (E)-2-[4-(Dimethylamino)phenyliminomethyl]-6-methylphenol. Acta Cryst., E63: o2902.

Gül ZS, Ersahin F, Agar E, Isik S (2007). (E)-2-[2-(Hydroxymethyl)phenyliminomethyl]-6-methylphenol. Acta Cryst., E63: o3547.

Gupta KC, Sutar AK. Polymer anchored Schiff base complexes of transition metal ions and their catalytic activities in oxidation of phenol. J. Mol. Catal. A: Chem., 272(1-2): 64-74. (2007).

Gupta KC, Sutar AK (2008). Catalytic activity of polymer anchored N,N′-bis (o-hydroxy acetophenone) ethylene diamine Schiff base complexes of Fe(III), Cu(II) and Zn(II) ions in oxidation of phenol. React. Funct. Polym., 68(1): 12-26.

Gutowski M, Chalasinski G (1993). Accuracy of the Boys and Bernardi function counterpoise method. J. Chem. Phys., 98(6): 4728-4738.

Hadjoudis E, Mavridis IM (2004). Photochromism and Thermochromism of Schiff Bases in the Solid State: Structural Aspects. Chem. Soc. Rev., 33(9): 579-588.

Hodnett EM, Mooney PD (1970). Antitumor activities of some Schiff bases. J. Med. Chem., 13(40: 786.

Valent A, Melník M, Hudecová D, Dudová B, Kivekäs R, Sundberg MR (2002). Copper(II) salicylideneglycinate complexes as potential antimicrobial agents. Inorg. Chim. Acta., 340: 15-20.

Jezierska-Mazzarello A, Vuilleumier R, Panek JJ, Ciccotti G (2010). Molecular property investigations of an ortho-hydroxy Schiff base type compound with the first-principle molecular dynamics approach. J. Phys. Chem. B., 114(1): 242-253.

Kelesoglu Z, Büyükgüngör O, Albayrak Ç, Odabasoglu M (2009). (E)-4-Methoxy-2-[3-(trifluoromethyl)phenyliminomethyl]phenol. Acta Cryst., E65: o3245-o3246.

Kluba M, Lipkowski P, Filarowski A (2008). Theoretical investigation of tautomeric equilibrium inortho-hydroxy phenyl Schiff bases. Chem. Phys. Lett., 463(4-6): 426-430.

Lee C, Yang W, Parr RG (1988). Development of the Colle-Salvetti correlation-energy formula into a functional of the electron density. Phys. Rev. B., 37(2): 785-789.

Lin YL, Gao J (2010). Internal proton transfer in the external pyridoxal 5'-phosphate Schiff base in dopa decarboxylase. Biochem., 49(1): 84-94.

Liu G, Peiliao J, Huang S, Lishen G, Qinyu R (2001). Fluorescence Spectral Study of Interaction of Water-soluble Metal Complexes of Schiff-base and DNA. Anal. Sci., 17(9): 1031-1036.

Nazir H, Yildiz M, Yilmaz H, Tahir MN, Ulku D (2000). Intramolecular hydrogen bonding and tautomerism in Schiff bases. Structure of N-(2-pyridil)-2-oxo-1-naphthylidenemethylamine. J. Mol. Struct., 524(1-3): 241-250.

Özdemir N, Dinçer M, Çukurovah A, Büyükgüngör O (2009). Experimental and theoretical investigation of the molecular and electronic structure of 5-(4-aminophenyl)-4-(3-methyl-3-phenylcyclobutyl)thiazol-2-amine. J. Mol. Model., 15(12): 1435-1445.

Pishkar L, Monajjemi M, Ilkhani AR, Mollaamin F (2010). Theoretical investigation of dielectric effects on nanostructure of β - amyloid peptide. Int. J. Phys. Sci., 5(9): 1450-1464.

Rodríguez-Córdoba W, Zugazagoitia JS, Collado-Fregoso E, Peon J (2007). Excited State Intramolecular Proton Transfer in Schiff Bases. Decay of the Locally Excited Enol State Observed by Femtosecond Resolved Fluorescence. J. Phys. Chem. A., 111(28): 6241-6247.

Rospenk M, Krol-Starzomska I, Filarowski A, Koll A (2003). Proton transfer and self-association of sterically modified Schiff bases. Chem. Phys., 287(1-2): 113-124.

Sahin ZS, Gümüs S, Macit M, Isik S (2009). (E)-2-[3-(Trifluoromethyl)phenyliminomethyl]benzene-1,4-diol. Acta Cryst., E65: o2754.

Sauer M, Yeung C, Chong JH, Patrick BO, MacLachlan MJ (2006). N-Salicylideneanilines: Tautomers for Formation of Hydrogen-Bonded Capsules, Clefts, and Chains. J. Org. Chem., 71(2): 775-788.

Schwenke DW, Truhlar DG (1985). Systematic study of basis set superposition errors in the calculated interaction energy of two HF molecules. J. Chem. Phys., 82(5): 2418-2427.

Snehalatha M, Ravikumar C, Hubert Joe I, Sekar N, Jayakumar VS (2009). Spectroscopic analysis and DFT calculations of a food additive Carmoisine. Spectrochim. Acta. A., 72(3): 654-662.

Taggi AE, Hafez AM, Wack H, Young B, Ferraris D, Lectka T (2002). The Development of the First Catalyzed Reaction of Ketenes and Imines: Catalytic, Asymmetric Synthesis of β-Lactams. J. Am. Chem. Soc., 124(23): 6626-6635.

Tanak H, Alpaslan BY, Yavuz M, Ağār E, Erşahinb F, Büyükgüngör O (2009). 2-[(2,4-Dimethylphenyl)iminomethyl]-3,5-dimethoxyphenol. Acta. Cryst., E65: o1572.

Tanak H, Yavuz M (2010). Density functional computational studies on (E)-2-[(2-Hydroxy-5-nitrophenyl)-iminiomethyl]-4-nitrophenolate. J. Mol. Model., 16(2): 235-241.

Tanak H, Yavuz M, Büyükgüngör O (2009). 2-Methyl-6-[2-(trifluoromethyl)phenyliminomethyl]phenol. Acta Cryst. E65: o2949.

Temel E, Albayrak Ç, Odabasoglu M, Büyükgüngör O (2007). (E)-3-[2-(Trifluoromethyl)phenyliminomethyl]benzene-1,2-diol. Acta. Cryst., E63: o374-o376.

Tezer N, Karakus N (2009). Theoretical study on the ground state intramolecular proton transfer (IPT) and solvation effect in two Schiff bases formed by 2-aminopyridine with 2-hydroxy-1- naphthaldehyde and 2-hydroxy salicylaldehyde. J. Mol. Model, 15(30): 223-232.

Tomasi J, Cammi R (1995). Remarks on the use of the apparent surface charges (ASC) methods in solvation problems: Iterative versus matrix-inversion procedures and the renormalization of the apparent charges. J. Com. Chem., 16(12): 1449-1458.

Toscano PJ, Marzilli LG (1984). B12 and Related Organocobalt Chemistry: Formation and Cleavage of Cobalt-Carbon Bonds. Prog. Inorg. Chem., 31: 105-204.

Upadhyay KK, Kumar A, Upadhyay S, Mishra PC (2008). Synthesis, characterization, structural optimization using density functional theory and superoxide ion scavenging activity of some Schiff bases. J. Mol. Struct., 873(1-3): 5-16.

Wang W, Zhang FX, Li J, Hu WB (2009). 2D conditional simulation of channels on wells using a random walk approach. Russ. J. Coord. Chem., 35(3): 429-437.

Ziółek M, Filipczak K, Maciejewski A (2008). Spectroscopic and photophysical properties of salicylaldehyde azine (SAA) as a photochromic Schiff base suitable for heterogeneous studies. Chem. Phys. Lett., 464(4-6): 181-186.